

STUDY OF SPH SIMULATION ON TUNNEL FACE COLLAPSE

Tsutomu Matsuo¹, Kunio Mori², Nobutaka Hiraoka², Mengxia Sun², Ha H.Bui³ and Ryoichi Fukagawa²

¹ Department of Technical Division, KFC, Ltd., Japan; ² Department of Civil Engineering, Ritsumeikan University, Japan; ³ Department of Civil Engineering, Monash University, Australia

ABSTRACT: Maintenance measures for tunnel portal zones have attracted increasing interest owing to the increased collapse risk of slopes by severe torrential rain and inland earthquakes in Japan in recent years. However, these large-scale collapse behaviours cannot be simulated by finite difference method (FDM) analysis. In this study, we applied the smoothed particle hydrodynamics (SPH) method to analyse the collapse behaviour of the tunnel face under construction and the effect of the stabilization method. First, we simulated the collapse behaviour at the tunnel portal zone by two-dimensional SPH simulation and compared it with an aluminium-bar experiment, and we showed that the SPH method is effective to model the overall tendency of the large deformation and the collapse behaviour in the experiments. Second, we simulated the collapse behaviour using the SPH method in the real tunnel portal zone collapse and provided a restraint result for collapse using facebolts. Therefore, we demonstrated that the SPH method is an effective technique to evaluate reinforcement measures.

Keywords: SPH, Aluminium-bar experiment, Collapse behaviour, Tunnel face, Tunnel portal zone

1. INTRODUCTION

Owing to the increased risk of natural disasters such as torrential rains or inland earthquakes, measures to ensure long-term stability during a tunnel's service life have assumed increasing importance in recent years. However, simulations of large-scale deformation of tunnel portals using the finite element method (FEM) and finite difference method (FDM) have yielded divergent results. Furthermore, an analytical technique to treat deformation from a small to a large scale to evaluate the effect of reinforcement measures remains lacking.

This study clarified the efficiency of the smoothed particle hydrodynamics (SPH) method in modelling the large-scale deformation and collapse behaviour of the tunnel portal zone.

First, we analysed the behaviour of collapse phenomena at the tunnel face using a two-dimensional SPH simulation and compared these results with those of aluminium-bar experiments. These efforts clarified that the SPH method is effective to simulate deformation from a small to a large scale as well as the collapse behaviour of the tunnel face. Second, we simulated the collapse behaviour using the SPH method in an example of real portal zone collapse. Furthermore, we proposed a method for analysing the effect of reinforcement measures and verified its effectiveness.

2. SPH OUTLINE AND APPROXIMATIONS [1]- [3]

The SPH method is a Lagrangian meshfree

method in which particles carry field variables such as mass, density, and stress tensor and move with the material velocity. By using the SPH method, the partial differential equations for the continuum are converted into the equations of motion of these particles. Other grid-based numerical methods such as FEM and FDM suffer from mesh distortion owing to large deformations. In contrast, SPH can handle large deformations, post-failure, and complex geometries very well, and it can model complex free surfaces without any special treatments.

The SPH method has recently been applied to solving large deformations and post-failure behaviour of geomaterials [4]- [7]. However, it has yet to be applied to the tunnel face collapse behaviour or evaluation of effectiveness of reinforcement measures on face stability.

In the SPH method, the computational domain is modelled using a set of discrete particles. The particles have a kernel function to define their interaction range, which is called the influence domain. The field variables are calculated using an interpolation process over its neighbouring particles located within the influence domain. The interpolation process is based on the integral representation of a field function $f(x)$ as follows:

$$\langle f(x) \rangle = \int_{\Omega} f(x') W(x - x', h) dx' \quad (1)$$

where x represents the particle location; Ω , the influence domain of the integral; W , the basis function of the approximation, which is called the kernel function; and h , the smoothing length, which defines the influence domain of W . The

approximation $\langle \cdot \rangle$ is called a kernel approximation.

The kernel function W must be chosen to satisfy the following three conditions: The first one is called the normalization condition:

$$\int_{\Omega} f(x')W(x-x',h)dx' = 1 \quad (2)$$

The second condition is called the delta function property; it should be satisfied when the smoothing length approaches zero:

$$\lim_{h \rightarrow 0} W(x-x',h) = \delta(x-x') \quad (3)$$

where $\delta(x-x')$ is a delta function. The third condition is called the compact support condition:

$$W(x-x',h) = 0 \quad \text{when } |x-x'| > kh \quad (4)$$

where k is a constant which specifies the non-zero region of the kernel function for an interpolation point. The choice of the kernel function in SPH directly affects the accuracy, efficiency and stability of the numerical algorithm. Many kernel functions have been proposed for SPH thus far. In this study, we apply the most popular cubic spline function proposed by Monaghan and Lattanzio [8], which has the following form:

$$W_{ij} = \alpha_d \times \begin{cases} 2/3 - R^2 + R^3/2, & 0 \leq R < 1 \\ (2-R)^3/6, & 1 \leq R < 2 \\ 0, & R \geq 2 \end{cases} \quad (5)$$

where α_d is the normalization factor, which is $15/(7\pi h^2)$ in two-dimensional space, and R is the normalized distance between particles i and j defined as $R = r/h$. The continuous integral representation (1) can now be discretized as a summation over the particles in the influence domain as follows:

$$\langle f(x) \rangle = \sum_{j=1}^N \frac{m_j}{\rho_j} f(x_j)W(x-x_j,h) \quad (6)$$

where $j = 1, 2, \dots, N$ indicate particles within the influence domain of the particle at x , the so-called neighbour; m_j and ρ_j are respectively the mass and density of particle j .

Figure 1 shows an approximation of this equation. The approximation for the spatial derivative $\nabla f(x)$ can be obtained simply by substituting $f(x)$ with $\nabla f(x)$ in equation (1). Integrating by parts and using the divergence theorem gives

$$\langle \nabla f(x) \rangle = \sum_{j=1}^N \frac{m_j}{\rho_j} f(x_j) \nabla W(x-x_j,h) \quad (7)$$

where $\nabla W(x-x_j,h)$ is a spatial derivative of $W(x-x_j,h)$. Further details of the SPH integration scheme can be found in [3] and [5].

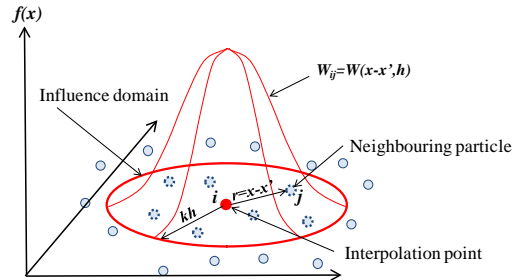


Fig. 1 Image of the SPH interpolation

3. EXPERIMENTAL STUDY ON COLLAPSE OF TUNNEL

3.1 Model of aluminium-bar experiment

We tested the behaviour at the time of the collapse of the tunnel face by the two-dimensional model experiment using aluminium bars and compared it with simulation by SPH analysis. Table 1 shows the experimental conditions. The tunnel height (D) is 8 cm with aluminium bars of two diameters, 1.6 mm and 3.0 mm, and 50-mm length, and two patterns of overburden, $H/D = 1.0$, and 2.0, are used. Figure 2 shows the initial condition of the aluminium-bar experiment.

Table 1 Specifications of aluminium-bar experiment

Items	Variable	Values
Total length	L	42 cm
Tunnel length	$L1$	12 cm
Tunnel height	D	8 cm
Overburden	H	8, 16 cm
(Ratio of H/D)	H/D)	(1.0), (2.0)

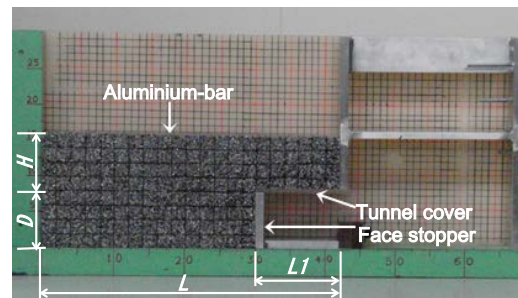


Fig.2 Initial condition of aluminium-bar experiment ($H/D=1.0$)

3.2 Analysis condition

We used the two-dimensional SPH method with the elastoplastic Drucker-Prager constitutive model and the nonassociated plastic flow rule to reproduce an aluminium-bar experiment. Table 2 shows the specifications of the simulation. The soil parameters, except for the unit weight, were similar to those measured by Umezaki et al. [9]. The unit weight of the soil model is $\gamma = 21.7 \text{ kN/m}^3$.

Figure 3 shows the simulation model. 2280 SPH particles were used to create the model with $H/D = 1.0$ shown in Fig.3, with an initial smoothing length of 6 mm. Table 2 shows the total number of particles in other cases. Free-roller boundary conditions with ghost particles [10] are used at the left and right ends, and full-fixity using virtual particles [5], [11] are used at the base and tunnel top. The initial stress condition is obtained by applying gravity loading to soil particles [5]. Then, the simulations are started by removing the face wall (A) in the side restriction shown in Fig.3.

Table 2 Specifications of SPH simulation

Items	Values
Unit weight	$\gamma = 21.7 \text{ kN/m}^3$
Young's modulus	$E = 5.84 \text{ MN/m}^2$
Poisson's ratio	$\nu = 0.3$
Cohesion	$c = 0 \text{ kN/m}^2$
Internal friction angle	$\phi = 21.9^\circ$

Note: Number of SPH particles is 3624 ($H/D = 2.0$)

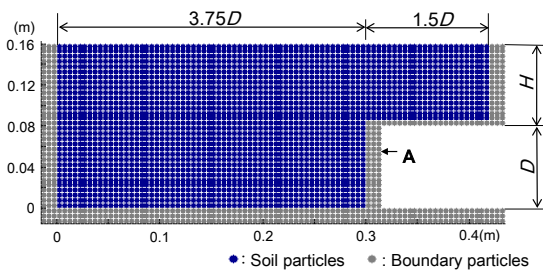


Fig. 3 SPH simulation model ($H/D = 1.0$)

3.3 Comparison between experiment and SPH

Figure 4 shows a comparison of the final configuration after collapse between the aluminium-bar experiment and simulation for $H/D = 1.0$ and 2.0 . The surface configurations in both the experiment and the SPH simulation shown in Fig.4 are straight for $H/D = 1.0$ and $H/D = 2.0$. The white dotted lines in Fig.4 indicate the boundary between the region of moved soils and nonmoved soils. These lines are equivalent to failure lines. The lines in the experiment and the simulation are similar for two H/D values. The failure lines in the

experiment are nearly straight for $H/D = 1.0$ and curved for $H/D = 2.0$.

These results clearly show that SPH analysis is effective to simulate the collapse of the tunnel face in the aluminium-bar experiments.

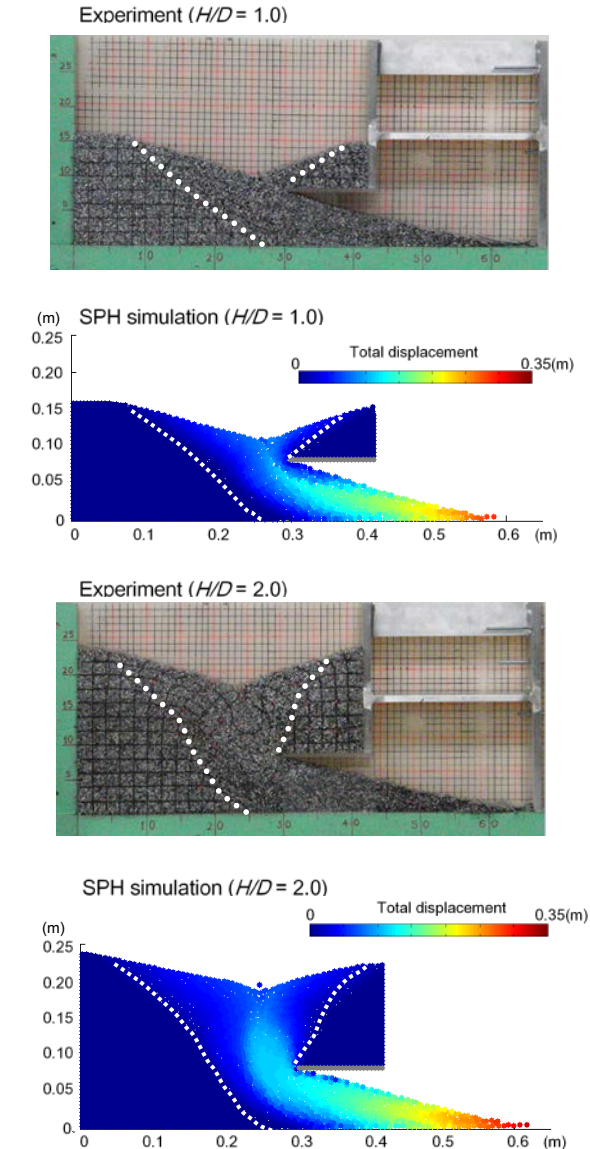


Fig.4 Comparison between SPH simulation and experiment for post-failure behaviour

4. SIMULATION ON A TUNNEL COLLAPSE EXAMPLE

4.1 Collapse process of tunnel

We tried to simulate a tunnel collapse, as shown in Photo 1, for a case of construction during torrential rains in Japan in 1995 [12], and provided a method for examining the efficacy of reinforcement by SPH. In this case, the tunnel and tunnel portal zone slope have collapsed.

The geology consists of layers of sandstone, tuff, and mudstone from the Neogene period. The water seeping into the ground owing to heavy rainfall caused the collapse of the tunnel face and the entire portal zone.

Figure 5 shows the collapse mechanism. The collapse process was as follows.



Photo 1 Overview of collapse of tunnel and tunnel portal zone [12]

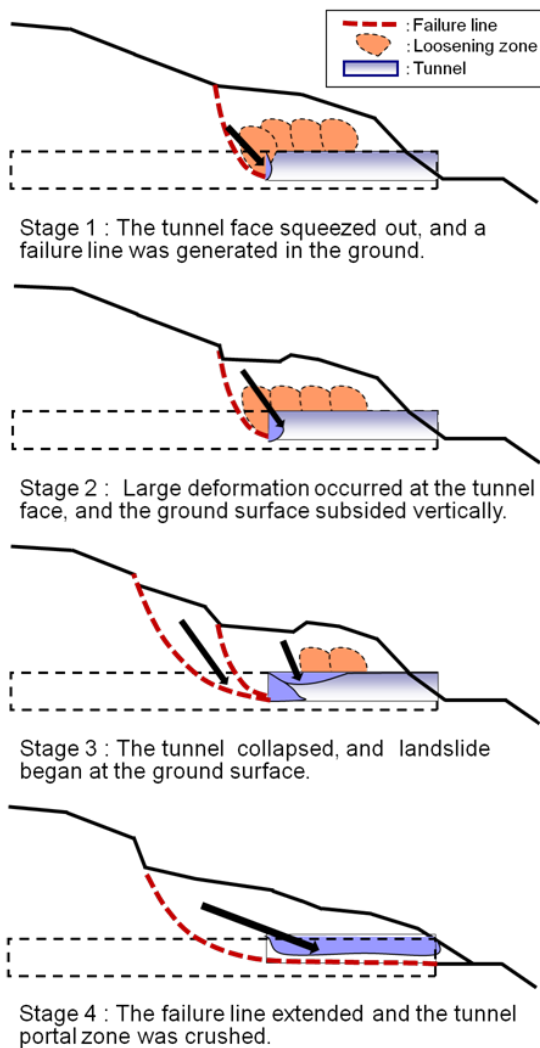


Fig.5 Process of tunnel collapse

Stage 1: The tunnel face squeezed out first and then, cracks were formed. A failure line was generated in the ground.

Stage 2: Flaking and falling off from the tunnel face and the crown of the tunnel occurred, and large deformation or beginning of failure occurred at the tunnel face. Concurrently, the ground surface subsided vertically.

Stage 3: The tunnel collapsed, and landslide began at the ground surface.

Stage 4: The failure line extended and the tunnel portal zone was crushed.

4.2 SPH Simulation

Figure 6 shows the analytical model and conditions of the SPH simulation. Figure 6 shows the size of the model and the soil parameters. The soil parameters are decided as follows: E , γ , ν , and ϕ values were set as those of unconsolidated soil that is common to Japan in reference to the parameters for numerical analysis [13]. Cohesion is decided based on the occurrence of failure through a parametric study by SPH, and this value is equivalent to the case of 10-m thickness of the landslide block [14]. A total of 7477 SPH particles were used to create the model with an initial smoothing length of 0.6 m.

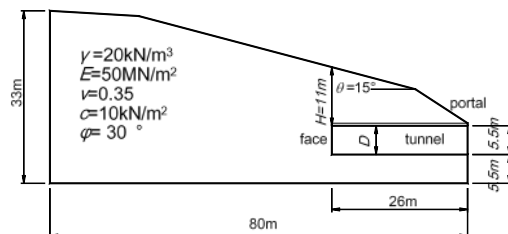


Fig.6 SPH model

Figure 7 shows a contour plot of the accumulated strain at 0.4 s and 0.8 s, which is the time just after the face collapse has started in the SPH simulation. Figure 7 shows that the failure line extends forward and upward from the bottom of the tunnel face, and the shear band extends from the top of the tunnel at the face to the ground surface vertically.

Figure 8 shows the post-collapse configuration by SPH simulation. Figure 8 shows that the maximum displacement is 6.8 m. It is also obvious that the failure line extending upward from the top of the tunnel reaches the ground surface, and subsidence occurs. Therefore, a second stage is simulated in the SPH, as shown in Fig.5 .

In real collapse, a landslide is caused by the crushing of the tunnel. In this simulation, the

cave-in of the crown is not considered. If we incorporate the conditions under which the cave-in of the crown occurs, it should be possible to simulate the real phenomena absolutely. However, it suffices to examine the efficacy of a reinforcement for verifying the reproducibility of early collapse behaviour by SPH.

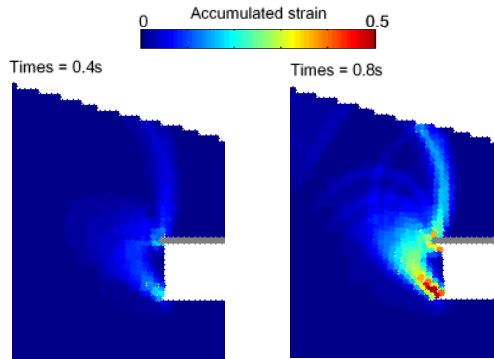


Fig.7 Contour plot of accumulated strain just after the face collapse has started

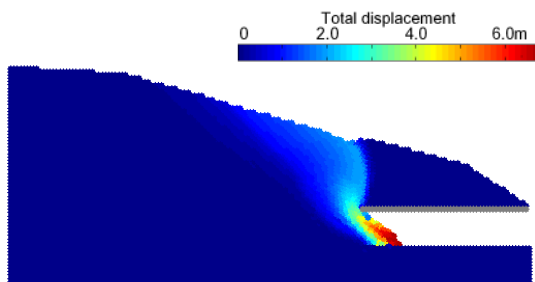


Fig.8 Final configuration after collapse

4.3 Analysis of face reinforcement

We modelled the face reinforcement using facebolts of 5-m length.

In this study, we describe the reinforcing works as the equivalent of Young's modulus and the shear strength with the cross-sectional performance of the material and ground. Figure 9 shows a facebolt model and the procedure to evaluate the properties of facebolts as parameters for analysis for the improved ground.

The cross-sectional area A_1 is assumed to be equal to A_0 of 0.5 m², which is multiplied by the initial spacing of SPH particle d of 0.5 m and unit width of 1.0 m. E_0 and c_0 are shown in Fig.6. We applied steel pipes with an outer/inner diameter of 76 mm/68 mm, as shown in Fig.9, for facebolts, and their properties are as follows: cross-sectional area A_s is 95 mm², Young's modulus E_s is 210 GN/m², and shear strength $\tau_s = 135$ MN/m². In addition, the distance between the bolts in the width direction a is set to 1.5 m.

According to the equations shown in Fig.9, the equivalent value E_1 is 320 MN/m² and c_1 is 180 kN/m² for the improved region. Table 3 shows the analysis case.

Figure 10 shows a contour plot of the relative strain as determined by SPH. Here, the relative strain is one divided by the maximum value of each case. The black particles denote those of the improved particles.

For one bolt, the displacement and strain are large and the tunnel face collapses. On the other hand, the displacements for two and three bolts are comparatively smaller. The time until the deformation converges is relatively short, being less than 1 s, and we could confirm that the face is stable.

However, particles attempt to inflow from the upper part of the tunnel face area, as indicated by a circle, in the case of two bolts. Therefore, three bolts are effective as a reinforcement.

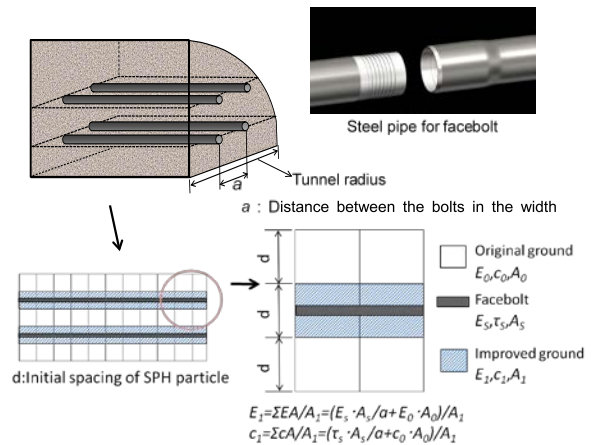


Fig.9 Model of facebolts

Table 3 Locations of facebolts

Number of bolts	Height from bottom (m)
1	3.8
2	2.3, 4.3
3	1.8, 3.3, 4.8

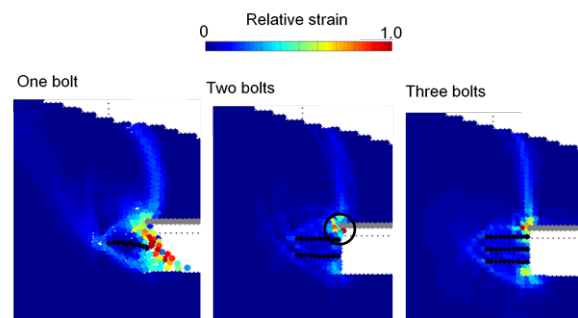


Fig.10 SPH results with facebolts

5. CONCLUSION

In this study, we applied the SPH method to examine tunnel collapse behaviour.

The results of our study are presented below.

- As an outline of the SPH method, we presented the basic formula of the SPH method and listed some details when this method is applied for simulating the ground deformation.
- Through a model experiment conducted using aluminium bars and SPH analysis, we simulated the collapse behaviour of the tunnel face and confirmed that the SPH simulation results are consistent with the experimental results. These results clearly demonstrate that SPH can be used to model the two-dimensional tunnel face collapse behaviour.
- We analysed a real case of collapse in a tunnel portal zone using the SPH method. We clearly demonstrated that the SPH method can sufficiently explain the real collapse phenomena.
- We modelled a case in which reinforcement works are installed in the tunnel face, and we confirmed the positive effect of this model for improving the stability of the face.

The SPH method used in this study can model large-scale deformations and separation behaviour that are difficult to handle using FEM or FDM and other grid-based continuum models. In addition, this method is easier to apply compared with discrete element method (DEM) and other discontinuum models.

As a future research agenda, we plan to advance further studies on the formulation of three-dimensional models for the detailed assessment and setting of external-force conditions when caused by earthquakes, rainfall, etc.

6. REFERENCES

- [1] Lucy L, "A numerical approach to testing the fission hypothesis", *Astronomical Journal*, Vol.82, 1977, pp.1031-1024.
- [2] Gingold RA and Monaghan JJ, "Smoothed particle hydrodynamics: theory and application to non-spherical stars", *Mon. Not. Roy. Astron. Soc.*, Vol.181, 1977, pp.375-389.
- [3] Bui HH, Fukagawa R, Sako K and Ohno S, "Lagrangian meshfree particles method (SPH) for large deformation and failure flows of geomaterial using elastic-plastic soil constitutive model", *International Journal for Numerical and Analytical Methods in Geomechanics*, Vol.32, 2008, pp.1537-1570.
- [4] Maeda K, Sakai H and Sakai M, "Development of seepage failure analysis method of ground with Smoothed Particle Hydrodynamics", *Journal of Structural and Earthquake Engineering*, JSCE, Division A, Vol.23, No.2, 2006, pp.307-319.
- [5] Bui HH, "Lagrangian mesh-free particle method (SPH) for large deformation and post-failure of geomaterials using elasto-plastic soil constitutive models", Ph.D. Dissertation, Ritsumeikan University, Japan, 2007.
- [6] Nonoyama H, Sawada K, Moriguchi S, Yashima A and Itoh K, "A 2D SPH simulation for real-scale slope excavation experiment", *Journal of JGS*, Vol.7, No.4, 2012, pp.543-555 (in Japanese).
- [7] Bui HH, Fukagawa R, Sako K, Okamura Y, "Earthquake induced slope failure simulation by SPH", *Fifth International Conference on Recent Advances in Geotechnical Earthquake Engineering and Soil Dynamics*, 2010.
- [8] Monaghan JJ and Lattanzio JC, "A refined particle method for astrophysical problems", *Astronomic and Astrophysics*, Vol.149, 1985, p.135-143.
- [9] Umezaki T, Kawamura T and Ochiai H, "Increment of confining pressure due to pullout of reinforcement and modelling of reinforcing mechanics", *Geosynthetic Engineering Journal*, Vol.120, 2005, pp.241-248 (in Japanese).
- [10] Libersky LD and Petschek AG, "Smoothed particle hydrodynamics with strength of materials", In *Proceedings of the Next Free Lagrange Conference*, Vol.395, 1991, pp.248-257.
- [11] Morris JP, Fox PJ and Zhu Y, "Modeling low Reynolds number incompressible flows using SPH", *Journal of computational physics*, Vol.136, 1997, pp.214-226.
- [12] Japan Tunneling Association: "Physiognomy guide for tunneling engineers No.6", *Tunnels and undergrounds*, Vol.43, No.10, 2012, p.50 (in Japanese).
- [13] Japan Railway Construction, Transport, and Technology Agency, "Standard design and construction of mountain tunnel", 2008, p.310 (in Japanese).
- [14] Japan Road Association, "Earth works on Road: Guiding principle on slope works and slope stability works", 2013, p.349 (in Japanese).

International Journal of GEOMATE, June, 2016, Vol. 10, Issue 22, pp. 2077-2082.

MS No.5357 received on June 15, 2015 and reviewed under GEOMATE publication policies. Copyright © 2015, Int. J. of GEOMATE. All rights reserved, including the making of copies unless permission is obtained from the copyright proprietors. Pertinent discussion including authors' closure, if any, will be published in Feb. 2017 if the discussion is received by Aug. 2016.

Corresponding Author: Tsutomu Matsuo
